Calorie restriction remodels gut microbiota and suppresses tumorigenesis of colorectal cancer in mice

XING-CHEN DAI[1-3*], YU-HUAN ZHANG[1-3*], YONG-LI HUANG[3], XIAO-TING WU[3],
YU-JIE FANG[3], YU-JING GAO[1,3,4] and FANG WANG[1,3]

[1]Department of Gastroenterology, General Hospital; [2]School of Clinical Medicine; [3]Key Laboratory of
Fertility Preservation and Maintenance of Ministry of Education, Department of Biochemistry and Molecular Biology,
School of Basic Medical Sciences; [4]National Health Commission Key Laboratory of Metabolic Cardiovascular
Diseases Research, Ningxia Medical University, Yinchuan, Ningxia 750004, P.R. China

Abstract. Colorectal cancer (CRC) is one of the most common cancers worldwide and the consumption of a high-calorie diet is one of its risk factors. Calorie restriction (CR) slows tumor growth in a variety of cancers, including colorectal cancer; however, the mechanism behind this remains unknown. In the present study, CR effectively reduced the tumor volume and weight in a xenograft BALB/c male nude mouse model. In addition, tumor immunohistochemistry revealed that the CR group had significantly higher expression of Bax (P<0.001) and significantly lower levels of Bcl2 (P<0.0001) and Ki67 (P<0.001) compared with control group. Furthermore, data from 16S ribosomal (r)RNA sequencing implied that CR was able to reprogram the microbiota structure, characterized by increased *Lactobacillus* constituent ratio (P<0.05), with amelioration of microbial dysbiosis caused by CRC. Further receiver operating characteristic curves demonstrated that the bacteria *Bacteroides* [area under the curve (AUC)=0.800], *Lactobacillus* (AUC=0.760) and *Roseburia* (AUC=0.720) served key roles in suppression of CRC in the mouse model. The functional prediction of intestinal flora indicated 'cyanoamino acid metabolism' (P<0.01), 'replication initiation protein REP (rolling circle plasmid replication)' (P<0.01), 'tRNA G10 N-methylase Trm11' (P<0.01) and 'uncharacterized protein with cyclophilin fold, contains DUF369 domain' (P<0.05) were downregulated in CR group. These findings implied that CR suppressed CRC in mice and altered the gut microbiota.

Introduction

Colorectal cancer (CRC) is one of the most common diseases globally, killing ~800,000 people each year (1). CRC has a complicated and varied etiology that is associated with risk factors, including environment, diet, living habits and genetic factors (2,3). In total, ≤90% of cancer cases are associated with lifestyle and the link between nutrition and CRC has received more attention (2).

The incidence of CRC is highest in economically developed countries and there is an increasing yearly trend in emerging countries, owing to increased consumption of high-calorie diets (4). Caloric restriction (CR) has been shown to suppress cell proliferation, increase apoptosis and lower the host inflammatory response; however, the underlying mechanism is uncertain (2,4).

The equilibrium of gut bacteria serves a key role in host physiological activities and dysbiosis of gut microbes can lead to conditions such as inflammatory bowel disease (IBD), irritable bowel syndrome, obesity, type 2 diabetes (5). The role of the microbiome in the development and progression of CRC has recently received increased attention; however, how the microbiota determines cancer susceptibility and progression remains unknown (6,7). Previous studies have investigated the connections between gut microbiota and CRC, in addition to the involvement of the microbiome in the development of CRC (8,9). Gut microbiota influence CRC susceptibility and advancement by influencing mechanisms such as inflammation and DNA damage, as well as excreting chemicals that promote or inhibit tumor formation (10).

The present study aimed to investigate the effects of CR on development of CRC and gut microbial diversity using a xenograft mouse model to determine the mechanisms by which CR suppresses tumorigenesis and the role of gut

Correspondence to: Professor Yu-Jing Gao, Key Laboratory of Fertility Preservation and Maintenance of Ministry of Education, Department of Biochemistry and Molecular Biology, School of Basic Medical Sciences, Ningxia Medical University, 1160 Shengli Street, Yinchuan, Ningxia 750004, P.R. China
E-mail: gaoyujing2004@126.com

Professor Fang Wang, Department of Gastroenterology, General Hospital, Ningxia Medical University, 804 Shengli South Street, Yinchuan, Ningxia 750004, P.R. China
E-mail: wangfang9803@163.com

*Contributed equally

microbial dysbiosis, thus, providing potential approaches for the prevention and treatment of CRC.

Materials and methods

Animals. A total of 10 specific-pathogen-free (SPF) grade BALB/c male nude mice (age, 4 weeks; body weight, 18-20 g) were obtained from Beijing Vital River Laboratory Animal Technology Co., Ltd. Mice were kept in an SPF environment (temperature 22±1˚C; humidity 40-60%) with a 12/12-h cycle of light and darkness with free access to food and drink. All animal procedures were authorized by the Ningxia Medical University Ethics Committee (approval no. 2021-045).

Reagents. RPMI-1640 medium (cat. no. AG29714278) was obtained from Hyclone (Cytiva). FBS (cat. no. 11011-8611) was purchased from Zhejiang Tianhang Biotechnology Co., Ltd. Penicillin-streptomycin (cat. no. ST488) and trypsin cell digestion solution (0.05% trypsin; cat. no. C0202) were purchased from Beyotime Institute of Biotechnology. Anti-Bax (cat. no. ab32503) and anti-Bcl2 (cat. no. ab32124) antibodies were purchased from Abcam. Anti-Ki67 antibody (cat. no. GB111499) was purchased from Wuhan Servicebio Technology Co., Ltd. Rabbit two-step detection (cat. no. PV-9001) and DAB color development kit (cat. no. ZLI-9018) were purchased from Beijing Zhongshan Golden Bridge Biotechnology Co., Ltd. BSA (cat. no. A8020) was purchased from Beijing Solarbio Science & Technology Co., Ltd.

Cell line and culture. The HCT116 human colon cancer cell line was obtained from Wuhan Procell Life Science & Technology Co., Ltd. (cat. no. CL-0096). The cells were grown in RPMI-1640 complete media (100 μg/ml streptomycin, 100 U/ml penicillin and 10% FBS) at 37˚C in a constant temperature incubator with 5% CO_2. The cells were trypsinized at 37˚C about 1 min after reaching 80-90% confluence and then passaged or used in the following experiments.

Xenograft mouse model and diet treatment. After one week of adaptive feeding, the 10 nude mice were subcutaneously implanted with $2x10^6/100 \mu$l HCT116 cells on the right flank. Every other day, tumor size was measured by a vernier caliper and the tumor volume was calculated using the formula $a^2xbx0.5$, where a is the shortest diameter and b is the diameter perpendicular to a (11). When the mean tumor volume of each nude mouse reached ~100 mm³ (12 days after subcutaneous tumor transplantation of mice), the mice were divided into the control group in nutrient-rich condition and the CR group in a nutrient-poor condition where subjects were fed with 70% of the usual food intake, with 5 animals in each group. The usual food intake for each group was calculated after monitoring for three consecutive days, using the random number table method (random.org) (12). Tumor size and health indicators, including body weight, feeding habits and locomotor activity were tracked every other day. The largest diameter of tumor size did not exceed 20 mm. Regardless of the size of the tumor, the mice were euthanized if they fulfilled the following prerequisites: i) Tumor position severely impaired usual body function; ii) tumor-associated pain or distress; iii) loss of >20% normal body weight; iv) ulceration or infection at tumor growth sites; and v) persistent self-mutilating behavior. None of the experimental animals reached the humane endpoints and were not euthanized before the end of the experiment. After 3 weeks, the mice were euthanized by inhalation of CO_2 gas (20% of the euthanasia chamber volume/min as a controlled flow rate of CO_2, which was increased to 100% of the euthanasia chamber volume/min once the mice were unconscious). Death was confirmed by cardiac and respiratory arrest, limb stiffness or dilated pupils. After mice were euthanized, the tumor masses were immediately dissected, weighed and fixed or preserved at -80˚C.

Immunohistochemistry (IHC) staining. After being fixed in 4% paraformaldehyde solution at 20-23˚C for 24 h and embedded in paraffin wax, tissue blocks were cut into 4 μm sections. These were deparaffinized in xylene and dehydrated in a series of ethanol concentrations (70, 80, 95 and 100% for 3 min each) at 20-23˚C. This was followed by citrate buffer antigen retrieval (after the solution was boiled, the microwave power was adjusted to 800 watts and continued heating for 2 min) and 5% BSA blocking at 20-23˚C for 30 min. Tissue sections were incubated with primary antibodies against Bax (1:250), Bcl-2 (1:250) and Ki67 (1:500) at 4˚C overnight. The following day, the tissue sections were returned to room temperature for 1 h followed by a 20 min incubation with secondary antibodies which were part of the Rabbit two-step detection kit at 37˚C. The tissue sections were stained using a DAB kit. The samples were dehydrated, made translucent, stained (20-23˚C) with hematoxylin (0.025%; 30 seconds) and sealed prior to light microscope (magnification, x40; Olympus Corporation; cat. no. BX53) observation for analysis. The staining standard was scored according to the intensity of cell staining as follows: i) No positive staining (negative, 0); ii) light yellow (weakly positive, 1); iii) brownish yellow (positive, 2) and iv) tan (strong positive, 3). The percentage of positive cells was divided into 4 grades: i) 1, ≤25%; ii) 2, 26-50%; iii) 3, 51-75% and iv) 4, >75%. The final score was obtained by multiplying the two scores (13,14).

16S ribosomal (r)RNA sequencing and data analysis. Intestinal contents of the mice (solid excreted feces or collected from the rectum and a small portion of semi-solid stool with relatively abundant water content that was at the end of the colon) were collected after mice were sacrificed. These samples were sent to Shanghai Personalbio Biotechnology Co., Ltd. for 16s rRNA sequencing and microbial community diversity composition analysis. DADA2 software (QIIME2 (version 2019.4)) was used for sequence denoising and the Vsearch software (version 2.13.4_linux_x86_64) was used for cluster analysis (15,16). After quality control which included the steps of primer removal, quality filtering, denoise, stitching, and removal of chimerism, the data were evaluated for bacterial species composition, α diversity (including Chao1, Observed, Shannon and Simpson indices) and β diversity (including the principal component analysis (PCA), principal coordinate analysis (PCoA) and non-metric multidimensional scaling analysis (NMDS)) and species differences using the QIIME2 (version 2019.4) gene cloud platform (https://www.genescloud. cn). Linear discriminant analysis effect size (LEfSe) analysis
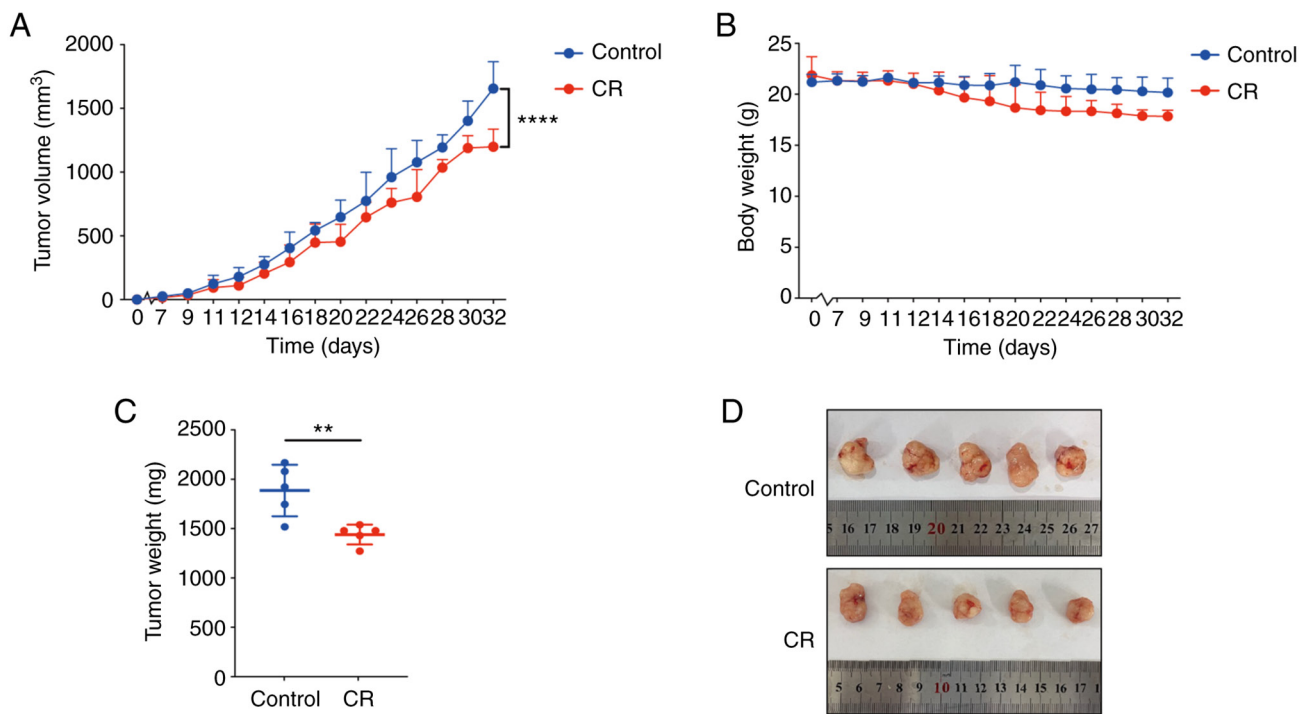
Figure 1. CR suppresses *in vivo* growth of CRC tumor. Changes in (A) tumor volume, (B) body mass, (C) tumor weight and (D) resected tumor samples from CRC solid tumor model mice. Data are presented as mean ± SD, n=5. **P<0.01, ****P<0.0001 vs. control. CR, calorie restriction; CRC, colorectal cancer.

was performed using gene cloud platform (genescloud.cn). Receiver operating characteristic (ROC) curve analysis was performed to with the XianTao tool (https://www.xiantao. love/products). Microbial functions were predicted by Phylogenetic investigation of communities by reconstruction of unobserved states (PICRUSt2; version 2.5.1; github. com/picrust/picrust) upon Kyoto Encyclopedia of Genes and Genomes (KEGG; kegg.jp/) databases and Clusters of Orthologous Genes (COG; ncbi.nlm.nih.gov/COG/) databases.

Statistical analysis. Unpaired Student's t test was used to compare differences in tumor volume and mass, mouse body weight, staining scores and species composition using Prism v9.0 software (GraphPad Software, Inc.). Sequence data analysis was performed using QIIME2 (version 2019.4) and R packages (version 3.2.0) (17). Kruskal-Wallis rank-sum and Dunn's post hoc test were used to examine differences between different sample groups. P<0.05 was considered to indicate a statistically significant difference. At least three independent biological replicates, and unless otherwise noted, all associated data are presented as mean ± SD.

Results

CR suppresses in vivo proliferation of CRC cells by regulating apoptosis and proliferation. In the present investigation, 10 mice were employed to examine the impact of CR on the *in vivo* development of CRC cells. The mean maximum diameter of tumor in CR and control group were 15.63±0.840 and 16.68±1.360 mm, respectively. The tumor volume in the CR group was significantly lower compared with the control group at 32 days (Fig. 1A and D). Similarly, the tumor mass was significantly reduced in mice of CR group compared with

the mice of control group (Fig. 1C). Notably, CR did not elicit a significant effect on the body weight of the mice (Fig. 1B).

In the present study, subcutaneous xenografts were subjected to IHC examination. Bax expression in the CR group was significantly increased (Fig. 2A-C), while Bcl-2 and Ki67 expression levels were significantly decreased compared with the control (Fig. 2D-I). The aforementioned results implied that CR was able to slow the progression of CRC xenografts by promoting apoptosis and suppressing proliferation.

CR increases the presence of gut microbiota in mice. Chao1, Observed, Shannon and Simpson indices were used to characterize bacterial species richness and diversity to thoroughly assess the changes in diversity of the microbial communities in CRC mice under CR circumstances (Fig. 3A). The CR group exhibited higher species abundance and community diversity than the control; however, this difference was not statistically significant.

The rank abundance curve revealed that the presence of gut microbiota in the CR group was not significantly different compared with the control (Fig. 3B). Rarefaction curve was used to determine whether the sequencing or sample volume was saturated (18). The rarefaction curves of all samples converged toward a plateau, indicating that all OTUs were sufficiently covered by the sequencing (Fig. 3C). The findings of rarefaction curve were in line with the α diversity index that CR increased the species diversity of the samples. The microbial abundance of the CR group was larger compared with the control at the same sequencing depth, showing that CR increased the abundance of gut microbiota in mice.

CR modifies the β diversity of gut microbiota. The PCA, PCoA and NMDS were used in the β diversity analysis. PCA,
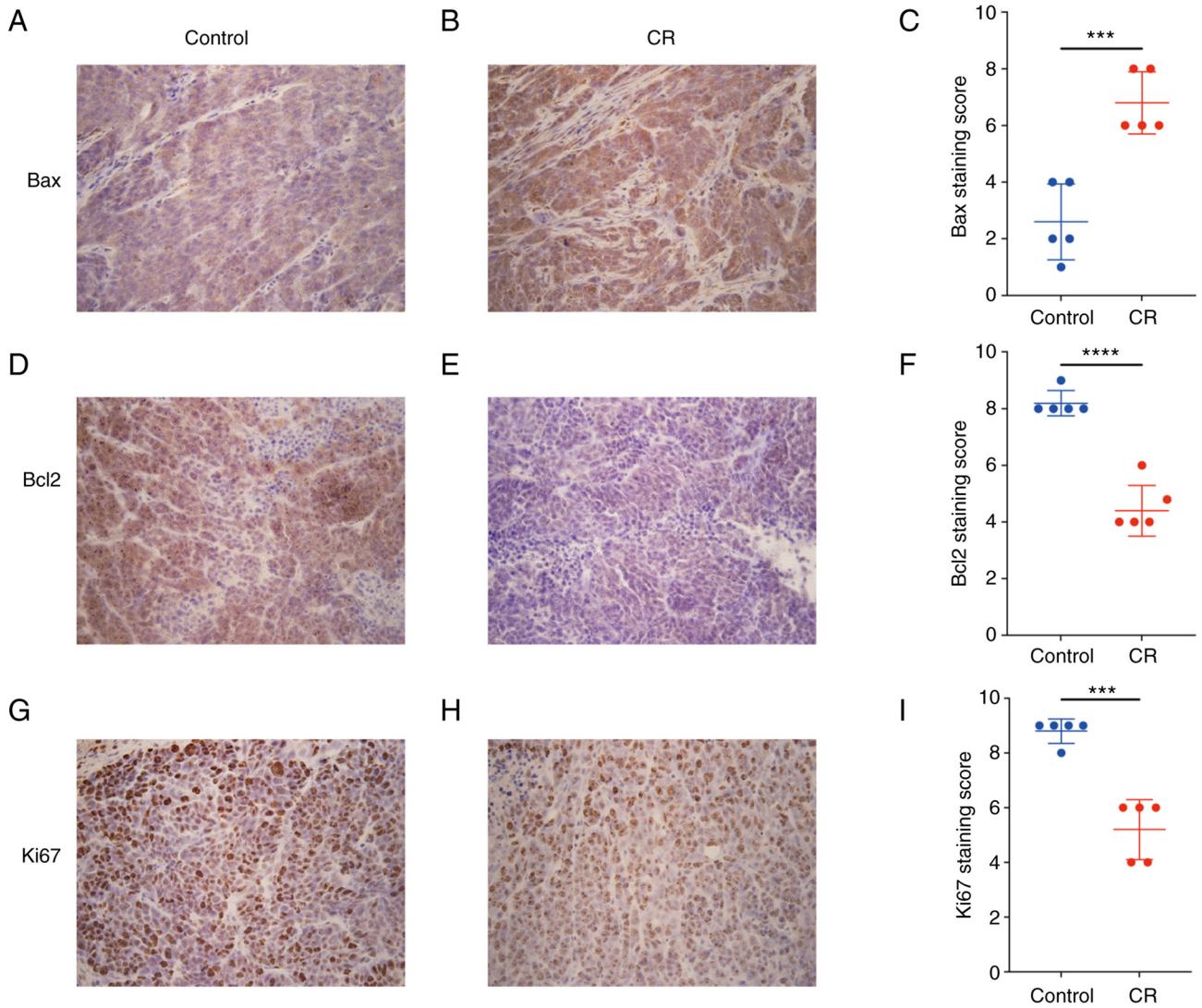
Figure 2. CR promotes apoptosis and inhibits proliferation of colorectal cancer cells. Immunohistochemical staining of genes associated with apoptosis or proliferation. Compared with (A) control group (A), the expression of Bax was increased in the CR group (B). (C) Staining score of Bax expression in each group, respectively. Compared with the control group (D), the expression of Bcl2 was decreased in the CR group (E). (F) Staining score of Bcl2 expression in each group, respectively. Compared with the control group (G), the expression of Ki67 was reduced in the CR group (H). (I) Staining score of Ki67 expression in each group, respectively. Magnification, x400. Data are displayed as mean ± SD, n=5. ***$P<0.001$, ****$P<0.0001$ vs. control. CR, calorie restriction.

using analysis of variance, was performed to detect the differences between multiple groups of data on a two-dimensional coordinate graph (Fig. 4A). To distinguish both groups stereoscopically, 3D-PCA plots were employed (Fig. 4B). PCoA was used to assess similarities or differences in data (Fig. 4C). NMDS was used to compare differences in bacterial community composition between sample groups based on the Bary-Curtis distance (Fig. 4D). The majority of the samples from the CR group were clustered together, according to PCA, 3D-PCA, and PCoA, whereas they were divided from the control group. Similar results were obtained using NMDS analysis. The closer proximity between each point, the more similar the sample compositions are. The matrices of the two groups were separated, except PCA (Fig. 4A), suggesting that CR caused alterations in the structure of the gut microbiota in CRC mice.

CR alters the composition of gut microbiota. To analyze phylogenetic or population genetics studies, the same mark (Sequences are divided into distinct OTUs according to a 97% similarity threshold, and each OTU is usually treated as a microbial species. A similarity of less than 97% was considered to belong to a different species, and a similarity of between 93 and 95% was considered to belong to a different genus.) is artificially set for a specific taxonomic unit (categories and groups, such as species, genus, family, order, class, phylum, and domain.), also known as the operational taxonomic unit (OTU) (19). OTU in each set were counted according to the grouping of samples and the Venn diagram was drawn to study which species were common and which were unique among different sample groups. Finally, a total of 18,626 OTUs were identified in the control group and 17,790 OTUs were found in the CR group, with the control and CR groups sharing a total of 2,886 OTUs (Fig. 5A).

Following comparison of the species composition of taxa at the phylum and genus levels in the fecal samples of CRC mice, discrepancies were discovered between the species compositions of the CR group and the control group
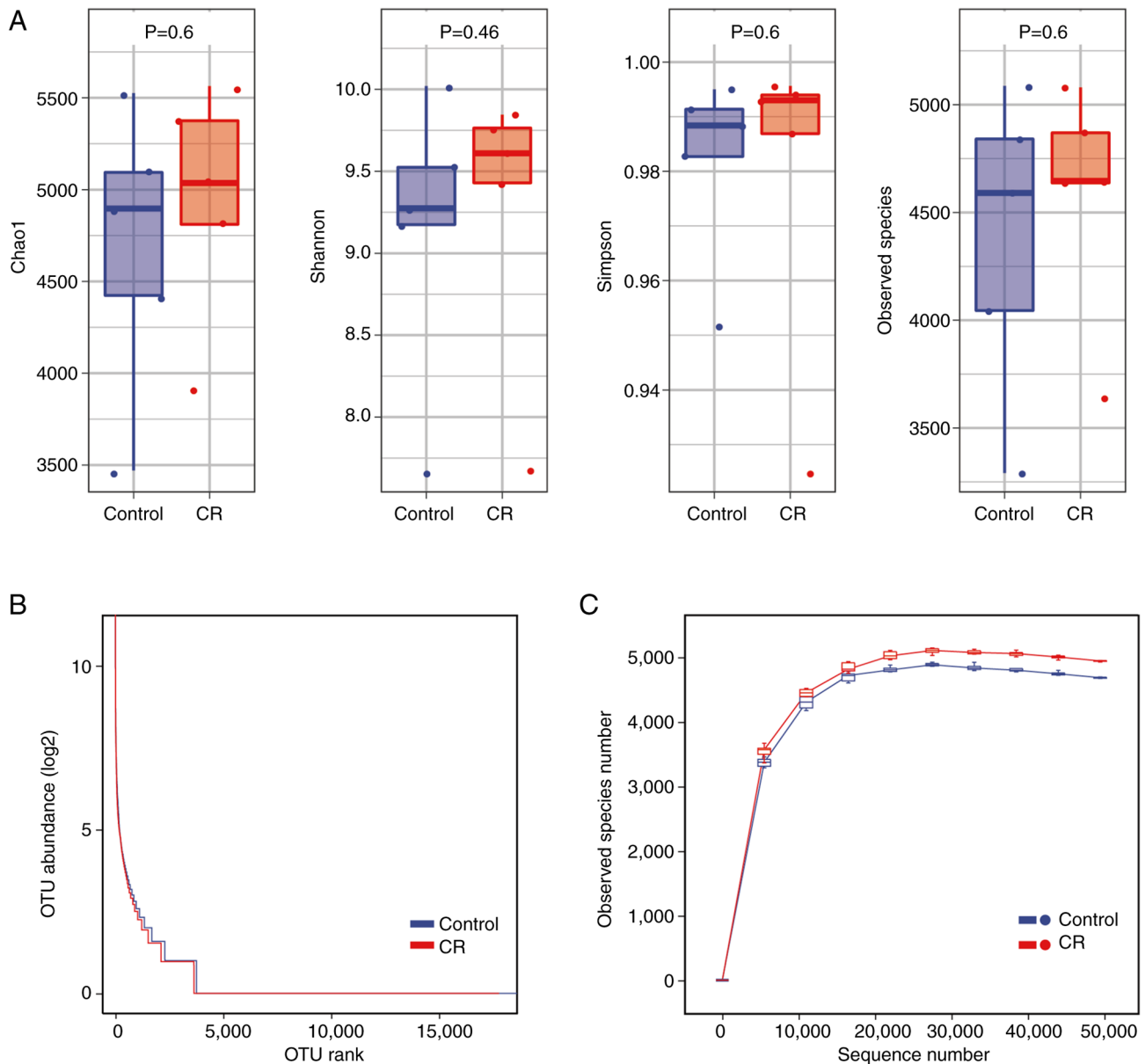
Figure 3. CR increases the presence of gut microbiota in mice. (A) Comparison of α diversity by Chao1, Shannon, Simpson and observed species index-based genus level. Data were analyzed using Kruskal-Wallis test. (B) Rank abundance. (C) Rarefaction curve. The ordinate of the rank abundance curve is the abundance value/mean value of each OTU in the sample/group following Log2 logarithmic transformation. Data are displayed as mean ± SD, n=5. CR, calorie restriction; OTU, operational taxonomic unit.

(Fig. 5B and C, E and F). *Firmicutes*, *Bacteroidetes* and *Verrucomicrobia* comprised the majority of the OTU at the phylum level; however, the differences in components between these two groups were not statistically significant. The OTU at the genus level was primarily composed of *Lactobacillus*, *Oscillospira*, *Ruminococcus* and *Akkermansia*. Moreover, the proportion of *Lactobacillus* in the CR group was significantly higher than that in the control. Subsequently, heat maps of species composition of mouse fecal samples at the phylum and genus levels were used to show species abundance in each group (Fig. 5D and G). *Proteobacteria*, *Chloroflexi*, *Gemmatimonadetes*, *Chlorobi*, *Acidobacteria*, *Armatimonadetes*, *Spirochaetes*, *OD1*, *Firmicutes* and *WS3* were upregulated in the CR group compared with the control. *Tenericutes*, *Deferribacteres*, *Actinobacteria*, *Fusobacteria*, *WPS-2*, *Verrucomicrobia*, Nitrospirae, *TM7*, *Bacteroidetes*

and *Cyanobacteria* were downregulated in the CR group at the phylum level (Fig. 5D). By contrast, at the genus level, *Oscillospira*, *Streptococcus*, *Ruminococcus*, *Anaeroplasma*, *Dehalobacterium*, *Ruminococcus*, *Prevotella*, *AF12*, *cc115*, *Akkermansia*, *Coprococcus*, *Bifidobacterium* and *Adlercreutzia* were downregulated in the CR group compared with the control group, whereas *Parabacteroides*, *Bacteroides*, *Roseburia*, *Alistipes*, *rC4-4*, *Lactobacillus* and *Candidatus arthromitus* were upregulated (Fig. 5G).

LEfSe was used to reveal species differences between samples within each group at all taxonomic levels to identify species with notable differences (20,21). Compared with the control group, the gut microbiota in the CR group had the highest abundance of *Chloroflexi* at the phylum levels and *Saprospirae* and *Anaerolineae* at the class levels (Fig. 6A and B). *Saprospirales*, *Rhodobacterales* and
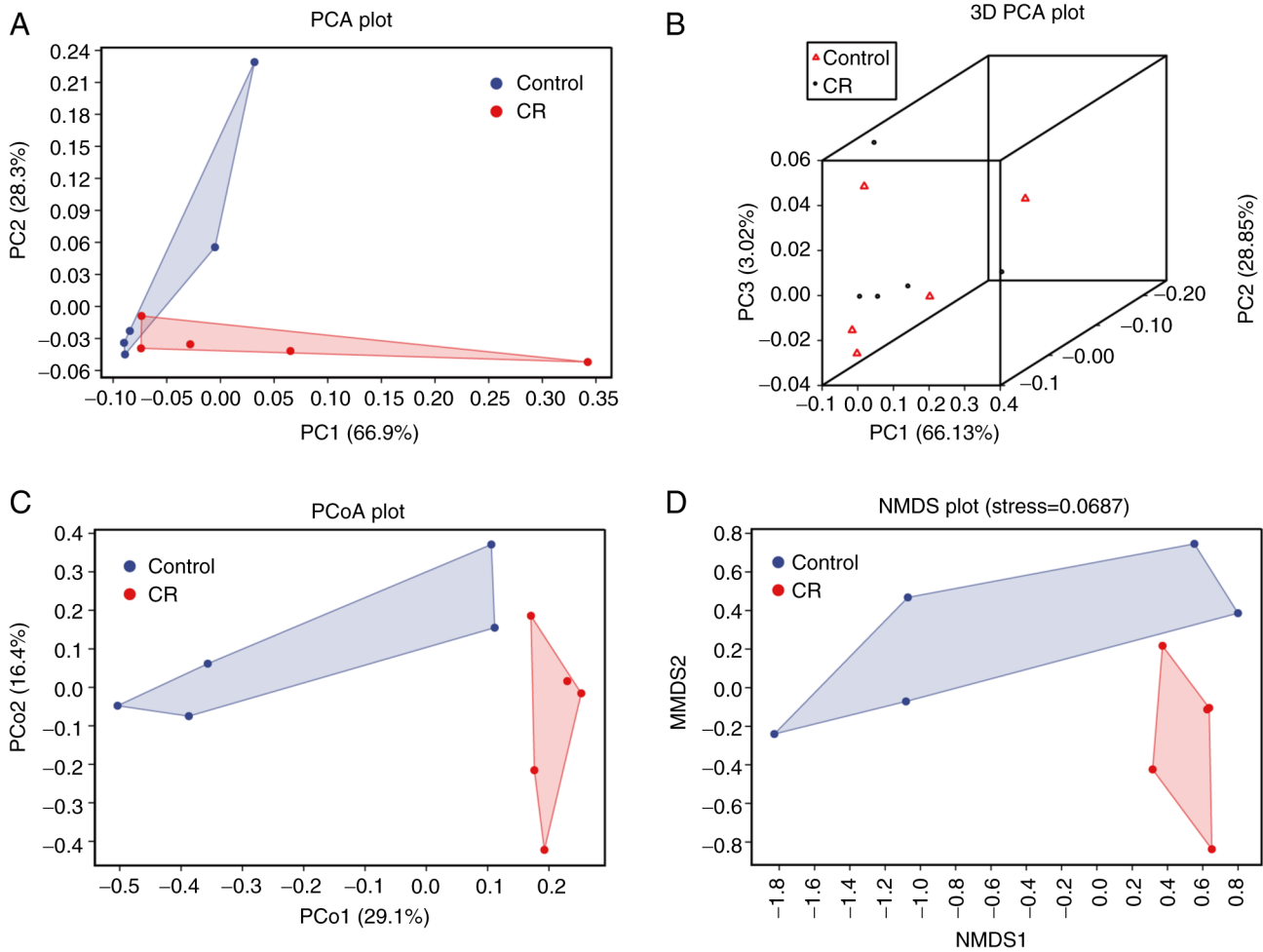
Figure 4. CR modifies β diversity of the gut microbiome. (A) PCA, (B) 3D PCA, (C) PCoA and (D) NMDS plot. The close proximity indicates that the sample compositions are similar. The percentages show how much of the distance matrix sample difference data each axis can explain. CR, calorie restriction; PCA, principal component analysis; PCoA, principal coordinate analysis; NMDS, non-metric multidimensional scaling.

Pasteurellales accounted for a higher proportion in the CR group at the order level, which was not the case in the control group. *Clostridiaceae*, *Peptococcaceae*, *Chitinophagaceae*, *Micrococcaceae*, *Porphyromonadaceae*, *Rhodobacteraceae*, *Pasteurellaceae* and *Streptomycetaceae* were more prevalent at the family level in the CR group compared with the control. By contrast with the control group, the enteric microorganisms of the CR group with higher abundance at the genus level were *Candidatus arthromitus*, *rc4-4*, *Aggregatibacter*, *Anaerostipes*, *Rothia*, *Rhodobacter*, *Parabacteroides*, *Streptomyces* and *Faecalibacterium*.

CR regulates key marker flora to interfere with CRC. Receiver operating characteristic (ROC) curve analysis is a widely used statistical analytic tool in medical research to assess the performance of diagnostic tests (22). In the present study, the species compositions of the control and the CR group were combined at the genus level to draw the ROC curve of bacteria and calculate the area under the curve (AUC) to determine which bacteria were regulated by CR (Fig. 7A and B). Analysis of the ROC curve revealed that *Bacteroides* (AUC=0.800), *Lactobacillus* (AUC=0.760) and *Roseburia* (AUC=0.720) had relatively high accuracy, indicating that CR may suppress CRC by controlling these bacteria.

Gene function prediction of gut microbiota. The 16S sequencing data was analyzed to identify the roles of bacterial genes (microbial genes after eliminating the host components) to explore the association between dysbiosis and CRC. KEGG) database was used to annotate the mouse fecal sample genes and a total of six categories and 33 subcategories of functional gene were discovered (Fig. 8A). There were four gene annotations associated with 'transport and catabolism' under cellular processes. In the environment classification, the most annotated topics were 'membrane transport' and 'signal transduction' with three each. 'Replication and repair' received more gene annotations than other categories, such as 'folding, sorting and degradation', 'Transcription' and 'Translation' in the genetic section, totaling six. The majority of human disease-associated genes in the gut microbiota of CRC under CR were associated with 'infectious diseases', with seven genes. Compared with other metabolism-associated genes, 'Carbohydrate metabolism' and 'xenobiotics biodegradation and metabolism' obtained more annotations, 17 and 15, respectively in metabolism classification, showing that the CR group had robust carbohydrate metabolism and gut microbiota capable of breaking down and metabolizing of foreign chemicals. 'Endocrine system' genes had the highest level of annotation across all organismal systems classification,
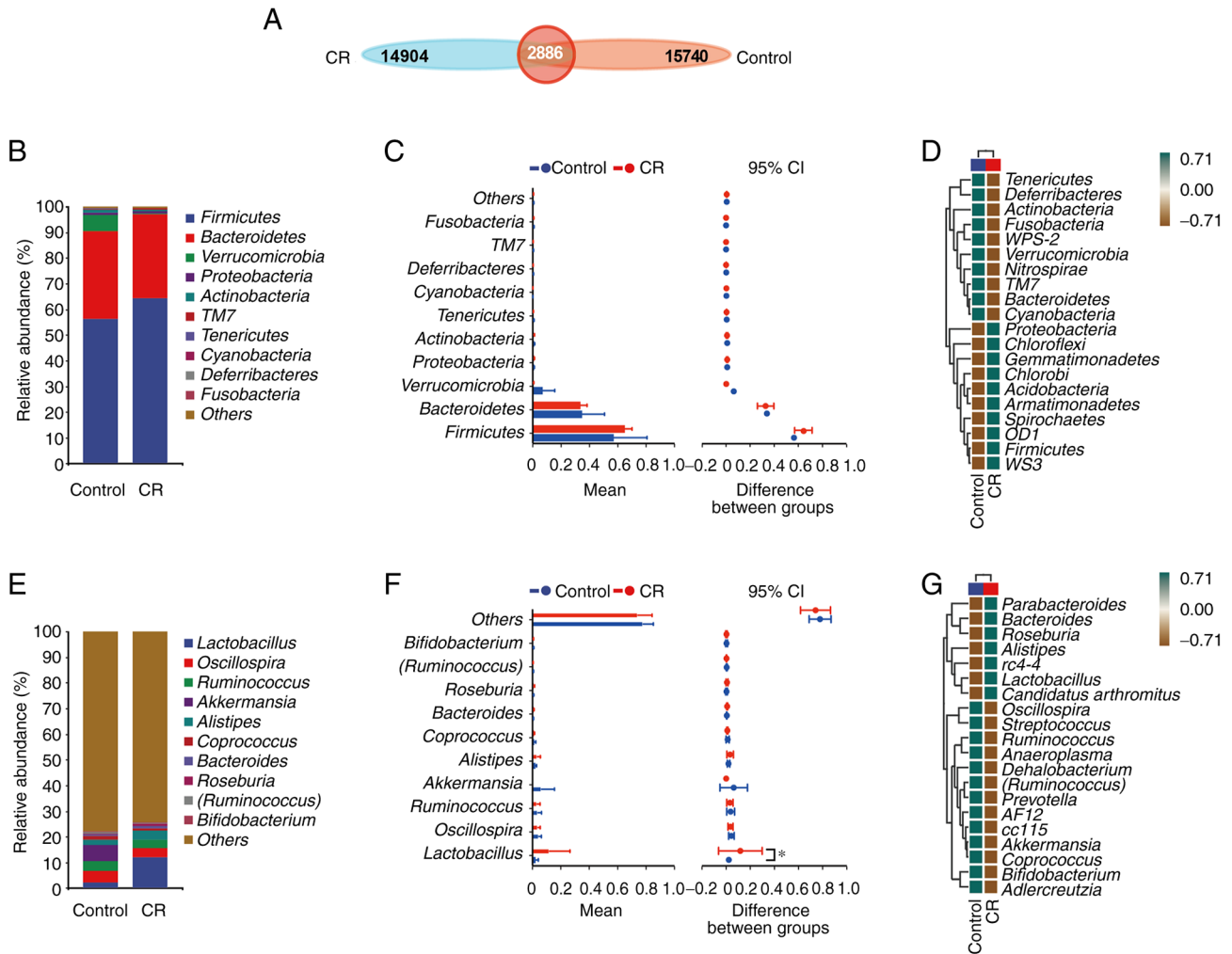
Figure 5. CR alters composition of gut microbiota. (A) Operational taxonomic unit Venn diagram of the intestinal flora. Relative abundances of species (B), species with differences (C), and heat map of species composition (D) at the phylum level in control and CR groups. At the genus level, each group's relative abundances of species (E), species with differences (F), and heat maps of species composition (G) are shown. Data are presented as mean ± SD, n=5. *P<0.05 vs. control. CR, calorie restriction.

suggesting that CR may maintain the stability of endocrine function in mice with CRC.

COG, a homologous protein annotation database established by National Center for Biotechnology Information (NCBI) to classify and assemble the encoded proteins of 21 entire genomes of bacteria, algae and eukaryotes, was used to analyze the associated COG pathways in the CR group (23). The COG database annotation results revealed that functional genes in CR mice fell into four primary categories and 25 subcategories (Fig. 8B). The findings revealed that 271 annotations were assigned to 'amino acid transport and metabolism'. The gut microbiota in the CR group had 214 genes annotated in 'Cell wall/membrane/envelope biogenesis', indicating that the gut microbiota biofilm creation was a major function. 'Defense mechanisms' made up 107 annotations in the CR group, showing that CR may aid colon cancer by increasing resistance to environment hazards. The functional characteristics of 851 gene annotations remained unclear.

The most substantially divergent pathways were identified by calculating the abundance values of KEGG and COG databases. The most downregulated pathway from the KEGG database in the CR group, compared with the control, was cyanoamino acid metabolism (pathway ID: ko00460; Fig. 8C). Based on COG database analysis, 'replication initiation protein REP (rolling circle plasmid replication) (pathway ID: COG5655), tRNA G10 N-methylase Trm11 (pathway ID: COG1041) and uncharacterized protein with cyclophilin fold, contains DUF369 domain' (pathway ID: COG2164) were the most downregulated categories in the CR group (Fig. 8D).

Discussion

Controlling dietary intake has been hypothesized to relieve physical and mental burdens associated with obesity (24). However, in recent years, an increasing number of studies has shown that CR provides patients with numerous other benefits in addition to weight loss (25,26). Choi et al (27) stated that CR allows the body to eliminate harmful cells while generating healthy new cells, therefore alleviating multiple sclerosis symptoms. Studies have conducted more in-depth investigations on how CR impacts the ability to perform these functions that assist in protecting the body against disease and maintaining health (28-32). In addition to the above-mentioned studies,
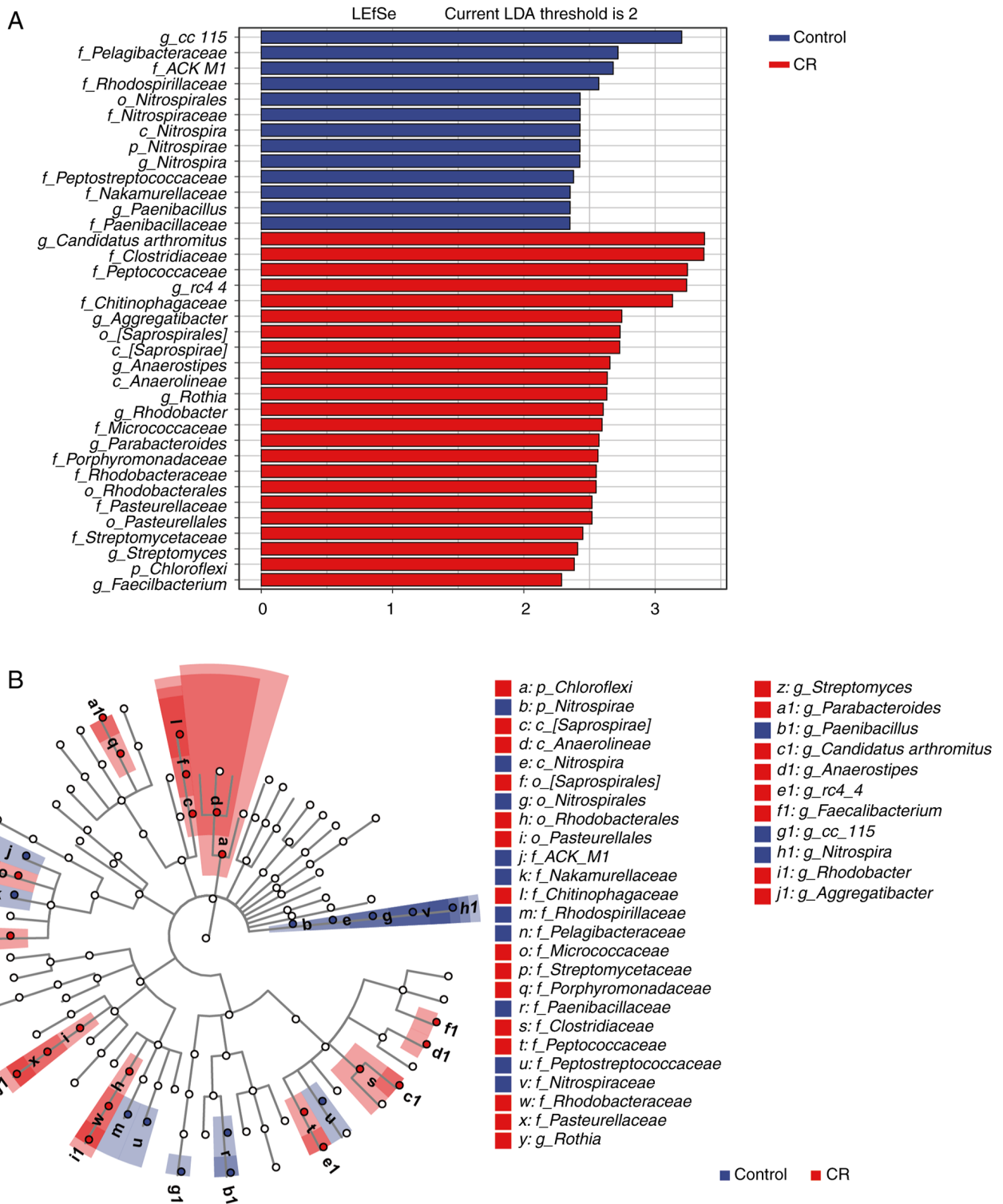
Figure 6. LEfSe study revealed that gut microbiota of the CR and control group vary at every level. (A) LDA score showed notable differences in the intestinal flora of mice in each group. (B) Taxonomic cladogram using the LEfSe method to show the phylogenetic distribution of fecal microbes associated with groups. The larger the LDA score, the greater the influence of species abundance on differences between groups. White nodes in the taxonomic cladogram depict taxa that do not differ between groups, while nodes that are colored represent differential taxa. The letters indicate taxa with differences between groups. The abundance is larger in the grouped samples. CR, calorie restriction; LEfSE, linear discriminant analysis effect size; LDA, logarithmic discriminant analysis.

Sbierski-Kind *et al* (33) showed that the gut microbiome is shaped by CR by reducing the levels of effector memory CD8+ T cells and memory B cells in mice , possibly postponing immunological senescence. However, the precise mechanisms behind this change are still unclear.

The transformation and absorption of nutrients in the human body is affected by intestinal microecology. Previous studies involving the use of metagenomics and bioinformatics technology in microecology have analyzed the structure and characteristics of intestinal microecology in various
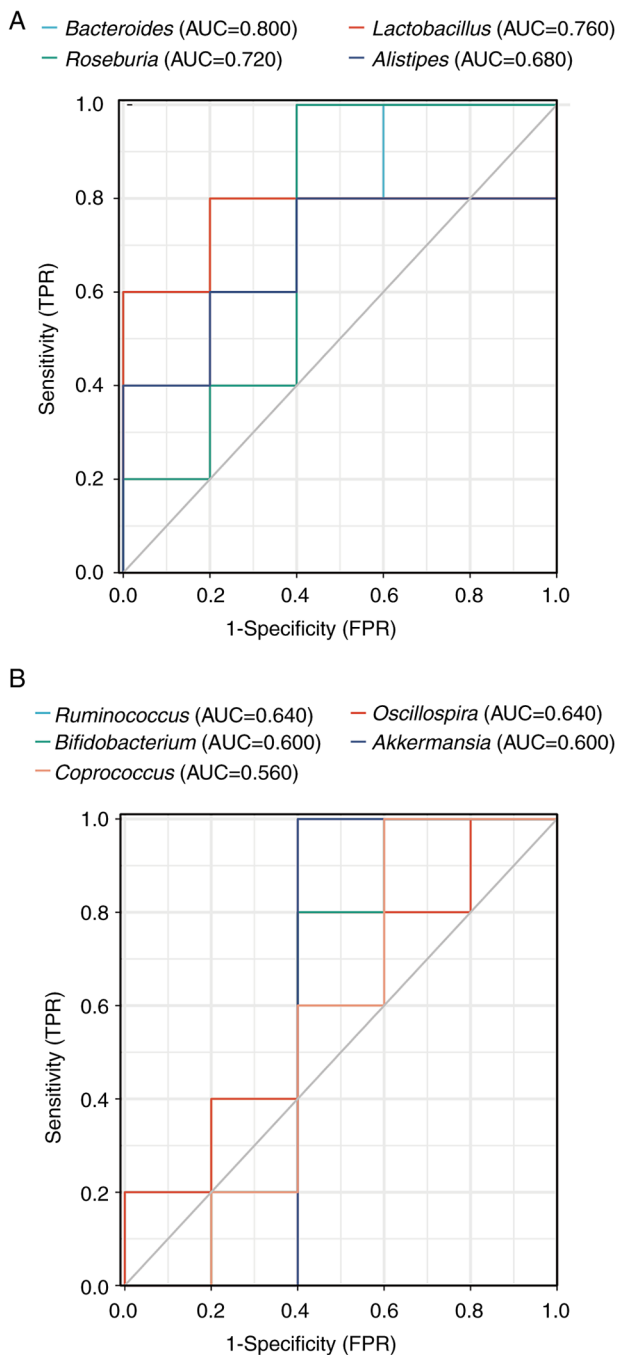
Figure 7. Evaluation of the predictive ability of microbiota markers for CRC in CR mice. Receiver operating characteristic analysis of representative differential (A) up- and (B) downregulated gut microbiota in the CRC model mice. The anticipated FPR was higher than the observed FPR. CRC, colorectal cancer; CR, calorie restriction; TPR, true positive rate; FPR, false positive rate.

of flora to discover meaningful markers to aid clinical research (37-39).

The present study found that CR decreased the volume and weight of subcutaneous CRC xenografts in mice by promoting CRC apoptosis while also inhibiting proliferation. The analysis of 16s rRNA sequencing on feces revealed CR markedly enhanced the abundance of gut microbiota in mice. In the normal gut microbiome, *Bacteroidetes* and *Firmicutes* are the most prevalent phyla, accounting for >80% of the gut microbiota (40). In addition, the *Firmicutes* to *Bacteroidetes* (F/B) ratio is an important indicator of dysbiosis in the gut microbiome (41-43). However, increased proportion of *Bacteroidetes* is considered to be advantageous to host health (44). Stojanov *et al* (45) revealed that the F/B ratio was greater in obese patients and markedly lower in patients with IBD). It has been proposed that *Firmicutes* bacteria extract energy from food more efficiently than *Bacteroidetes*, resulting in more efficient calorie absorption and consequent increased weight gain (46). However, *Firmicutes* is negatively connected with gut immune factors and antimicrobial peptides and positively correlated with inflammatory proteins and oxidative stress parameters, as Xia *et al* (47). Magne *et al* (46) showed that *Bacteroidetes* produces mostly acetate and propionate, while *Firmicutes* produces more butyrate, a health-promoting molecule shown to optimize insulin sensitivity, exert anti-inflammatory activity, regulate energy metabolism and increase leptin gene expression (48). In the present study, *Firmicutes* was notably increased in the CR group at the phylum level, whereas *Bacteroidetes* was notably decreased; this increase in the F/B ratio in the CR group may indicate that CR led to changes in the mouse gut microenvironment that were not detrimental to the mice.

Akkermansia is the most pervasive *Verrucomicrobia* species observed in humans and high-fat and high-calorie meals enhance the presence of *Akkermansia* (49,50). *Verrucomicrobia* has also been shown to promote regulatory immunity (51), making it a target for gut microbial intervention to improve regulatory immunity. Wu *et al* (52) demonstrated that interleukin-6 knockout mice possess markedly changed gut microbiota diversity than wild-type C57BL/6J mice, which included a decrease in the presence of *Firmicutes* at the phylum level and *Lactobacillus* at the genus level but an increase in *Verrucomicrobia* at the phylum level and *Akkermansia* at the genus level. Despite the absence of statistical significance in the present study, it was noted that CR mice had lower levels of *Verrucomicrobia* at the phylum level and decreased *Akkermansia* at the genus level. Additional studies into the association between these aforementioned changes in the flora caused by CR and the immunity of the organism are still required.

The *Lactobacillus* genus is a group of microorganisms that live in the body and benefit the host health. Previous research has identified that oral preparations containing *Lactobacillus* strains restore intestinal barrier function and immune markers and decrease systemic inflammation and/or cancer progression (53,54). Lin *et al* (55) showed that probiotics, including *Lactobacillus* and *Bifidobacterium*, prevent CRC growth by decreasing inflammation and angiogenesis, as well as improving function of the intestinal barrier by secreting short-chain fatty acids. In the present research,

populations, resulting in a body of research on the association between intestinal microecology and tumors (34,35). Gut microbiota crosstalk with innate and acquired immune cells has been shown to enhance the intermediate effects of innate immune cells, antitumor effect of acquired immune cells and tumor immunogenicity of cells, thereby reprogramming tumor microenvironment immunity and improving the immune checkpoint inhibitor response (36). Additional studies have investigated changes in the richness and percentage
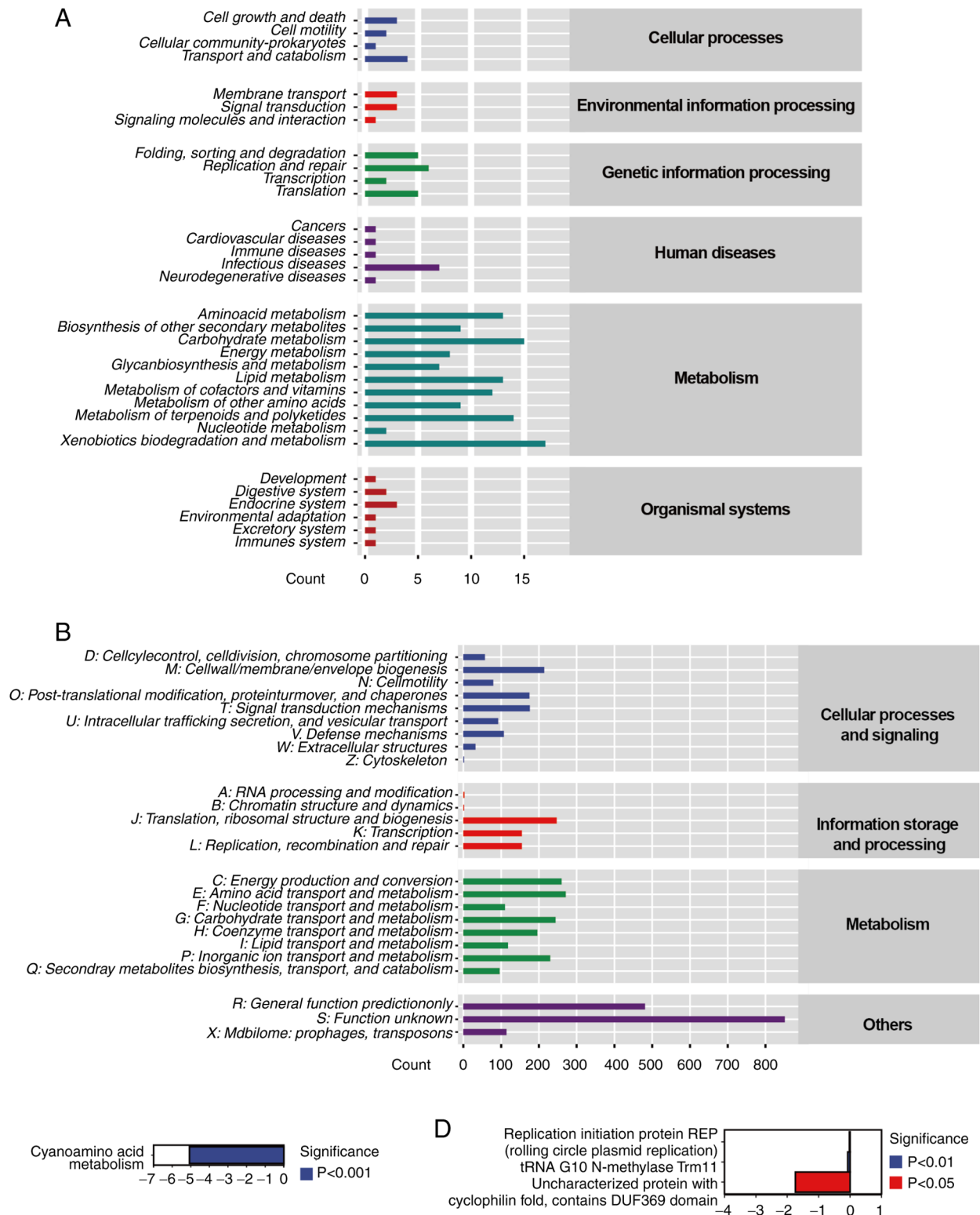
Figure 8. Gene function prediction of gut flora. (A) KEGG and (B) COG functional pathways and counts of gut microbiota in the CR group. First-level pathways/classifications are mean abundance of all samples. Metabolic pathways with notable differences between groups in (C) KEGG and (D) COG pathway. The positive value of log2(fold-change) on the x-axis represents the up-regulation compared with the control group. The negative value is downregulation compared with the control group. CR, calorie restriction; KEGG, Kyoto Encyclopedia of Genes and Genomes; COG, Clusters of Orthologous Genes; AUC, area under the curve.

a notable increase in *Lactobacillus* was discovered in CR mice, with AUC=0.760, indicating that CR may improve the intestinal barrier function of mice and effectively control the inflammatory response, thus inhibiting CRC growth.

In the present study, levels of *Bacteroides* and *Roseburia* in the CR group were higher compared with the control. *Bacteroidetes* species are constituents of the *Bacteroidetes* phylum, with the genus *Bacteroidetes* containing the most

common *Bacteroidetes* species in the human gut (56). *Bacteroidetes* produce butyrate and induce regulatory T cell development, both of which decrease inflammation (57). *Bacteroides* levels are considerably lower in obese children and teenagers and are inversely associated with low-density lipoprotein cholesterol in the blood, waist circumference and BMI (58,59). *Roseburia* is a Gram-positive, anaerobic, butyrate-producing bacterium that was originally isolated from human excrement and belongs to the *Firmicutes* phylum (60). *Roseburia* is detected in low abundance in numerous intestinal disorders, implying that the bacteria serve a vital function in maintaining intestinal homeostasis, such as generating short-chain fatty acids (61). Furthermore, compared with the general population, the presence of *Roseburia* is negligible in patients with inflammatory bowel illness such as ulcerative colitis and Crohn's disease (62,63). The increase in *Bacteroides* and *Roseburia* in the CR group suggests that the ability of CRC mice to maintain intestinal homeostasis improved and CR may have altered the gut microbial environment of CRC mice, enhancing immunological function and exerting anti-tumor effects. However, our study used a right flank site xenograft tumor model rather than a CRC model in situ in the intestine, thus more studies are needed to corroborate our hypothesis.

Although microbiota genome information was not established, 16S sequencing data was analyzed using PICRUSt to identify the potential functions of the microbiota genes. With only the sequencing data of microbiota marker genes, the known microbial genome data was used to forecast the composition of microbiota genes or functional units for intestinal microbiota according to 16S rRNA sequencing results (64). KEGG and COG databases were used to identify the potential functions of associated metabolic pathways. The metabolism of cyanoamino acids leads to an increase in the metabolism and production of intracellular signaling molecules and proteins, as well as the creation of biofilms (65). In gastric cancer, cyanoamino acid metabolism is disturbed and disorganized, which primarily manifests as upregulation of glycine levels and the downregulation of alanine levels (66,67). The downregulation of cyanoamino acid metabolism in the CR group may contributes to a better understanding of the underlying mechanisms of CRC . In the present study, replication initiator protein REP (rolling circle plasmid replication), tRNA G10 N-methylase Trm11 and uncharacterized protein with cyclophilin fold proteins were all found to be downregulated in the CR group. Rolling circle replication (RCR) is a replication initiation mechanism used by plasmids of certain Gram-negative bacteria (68). tRNA G10 N-methylase Trm11 protein is ubiquitous in archaea and eukaryotes (69). The enrichment of these gene annotations contributes to understanding of the mechanism by which CR serves a role in suppressing CRC and regulating gut microbiota.

There are limitations to the present study. Previous studies have shown that gut dysbiosis serves a key role in the development, progression and response to the treatment of CRC (70-72). Therefore, it can be concluded that remodeling of gut microbiota contributes to the suppressive effect of CR on CRC development in the mice. However, a cause-effect investigation is required to determine the key functions and mechanisms of gut bacteria in the regulation of CRC by CR in future. In addition, intestinal mucosa is a dynamic environment where the host continually interacts with trillions of commensal microorganisms and sporadically interacts with pathogens (73). The present study failed to collect the microorganisms from the intestinal mucosa to analyze the intestinal transit bacteria due to technical limitations. It is hypothesized that examining the bacteria in the gut mucosa will support the present results.

In conclusion, the present study revealed that CR modified gut microbiota and inhibited CRC growth by regulating apoptosis and proliferation of CRC cells in a mouse model. CR increased the proportions of beneficial bacteria, such as *Lactobacillus*, which may provide a novel approach to treating CRC by CR-induced remodeling of gut microbiota. As studies on gut microbiota increase, it is anticipated that the development of a new food culture centered on low-calorie diet may assist in preventing and controlling the progression of CRC.

Acknowledgements

Not applicable.

Funding

Availability of data and materials

The datasets generated and/or analyzed during the current study are available in the NCBI Sequence Read Archive repository (accession no. PRJNA890426; ncbi.nlm.nih.gov/bioproject/PRJNA890426).

Authors' contributions

XCD and YHZ wrote the draft of the manuscript. XCD, YHZ and YLH conducted the experiments. XCD, YHZ, YLH, YJF and XTW collected and analyzed the data. YJG and FW designed and supervised the study, and revised the manuscript. All authors have read and approved the final manuscript. YJG and FW confirm the authenticity of all the raw data.

Ethics approval and consent to participate

The Animal Experimental Ethics Committee of Ningxia Medical University (Yinchuan, China) approved this study (approval no. 2021-045).

Patient consent for publication

Not applicable.

Competing interests

The authors declare that they have no competing interests.

References

1. Siegel RL, Miller KD, Sauer AG, Fedewa SA, Butterly LF, Anderson JC, Cercek A, Smith RA and Jemal A: Colorectal cancer statistics, 2020. CA Cancer J Clin 70: 145-164, 2020.
2. Tammariello AE and Milner JA: Mouse models for unraveling the importance of diet in colon cancer prevention. J Nutr Biochem 21: 77-88, 2010.
3. Currais P, Rosa I and Claro I: Colorectal cancer carcinogenesis: From bench to bedside. World J Gastrointest Oncol 14: 654-663, 2022.
4. Hursting SD, Lavigne JA, Berrigan D, Perkins SN and Barrett JC: Calorie restriction, aging, and cancer prevention: Mechanisms of action and applicability to humans. Annu Rev Med 54: 131-152, 2003.
5. Bull MJ and Plummer NT: Part 1: The human gut microbiome in health and disease. Integr Med (Encinitas) 13: 17-22, 2014.
6. Clay SL, Fonseca-Pereira D and Garrett WS: Colorectal cancer: The facts in the case of the microbiota. J Clin Invest 132: e155101, 2022.
7. Khosravi AD, Seyed-Mohammadi S, Teimoori A and Dezfuli AA: The role of microbiota in colorectal cancer. Folia Microbiol (Praha) 67: 683-691, 2022.
8. Bradbury KE, Murphy N and Key TJ: Diet and colorectal cancer in UK Biobank: A prospective study. Int J Epidemiol 49: 246-258, 2020.
9. Bullman S, Pedamallu CS, Sicinska E, Clancy TE, Zhang X, Cai D, Neuberg D, Huang K, Guevara F, Nelson T, *et al*: Analysis of fusobacterium persistence and antibiotic response in colorectal cancer. Science 358: 1443-1448, 2017.
10. Sanchez-Alcoholado L, Laborda-Illanes A, Otero A, Ordóñez R, González-González A, Plaza-Andrades I, Ramos-Molina B, Gómez-Millán J and Queipo-Ortuño MI: Relationships of gut microbiota composition, short-chain fatty acids and polyamines with the pathological response to neoadjuvant radiochemotherapy in colorectal cancer patients. Int J Mol Sci 22: 9549, 2021.
11. Ren J, Ding L, Zhang D, Shi G, Xu Q, Shen S, Wang Y, Wang T and Hou Y: Carcinoma-associated fibroblasts promote the stemness and chemoresistance of colorectal cancer by transferring exosomal lncRNA H19. Theranostics 8: 3932-3948, 2018.
12. Toivonen RK, Emani R, Munukka E, Rintala A, Laiho A, Pietilä S, Pursiheimo JP, Soidinsalo P, Linhala M, Eerola E, *et al*: Fermentable fibres condition colon microbiota and promote diabetogenesis in NOD mice. Diabetologia 57: 2183-2192, 2014.
13. Guo Z, Zhang X, Zhu H, Zhong N, Luo X, Zhang Y, Tu F, Zhong J, Wang X, He J and Huang L: TELO2 induced progression of colorectal cancer by binding with RICTOR through mTORC2. Oncol Rep 45: 523-534, 2021.
14. Wang F, Wu X, Li Y, Cao X, Zhang C and Gao Y: PFKFB4 as a promising biomarker to predict a poor prognosis in patients with gastric cancer. Oncol Lett 21: 296, 2021.
15. Callahan BJ, McMurdie PJ, Rosen MJ, Han AW, Johnson AJ and Holmes SP: DADA2: High-resolution sample inference from Illumina amplicon data. Nat Methods 13: 581-583, 2016.
16. Rognes T, Flouri T, Nichols B, Quince C and Mahé F: VSEARCH: A versatile open source tool for metagenomics. PeerJ 4: e2584, 2016.
17. Bolyen E, Rideout JR, Dillon MR, Bokulich NA, Abnet CC, Al-Ghalith GA, Alexander H, Alm EJ, Arumugam M, Asnicar F, *et al*: Reproducible, interactive, scalable and extensible microbiome data science using qiime 2. Nat Biotechnol 37: 852-857, 2019.
18. Nipperess DA and Matsen FA IV: The mean and variance of phylogenetic diversity under rarefaction. Methods Ecol Evol 4: 566-572, 2013.
19. Edgar RC: UPARSE: Highly accurate OTU sequences from microbial amplicon data. Nat Methods 10: 996-998, 2013.
20. Rastelli E, Corinaldesi C, Dell'Anno A, Tangherlini M, Martire ML, Nishizawa M, Nomaki H, Nunoura T and Danovaro T: Drivers of bacterial alpha- and beta-diversity patterns and functioning in subsurface hadal sediments. Front Microbiol 10: 2609, 2019.
21. Segata N, Izard J, Waldron L, Gevers D, Miropolsky L, Garrett WS and Huttenhower C: Metagenomic biomarker discovery and explanation. Genome Biol 12: R60, 2011.
22. Obuchowski NA and Bullen JA: Receiver operating characteristic (ROC) curves: Review of methods with applications in diagnostic medicine. Phys Med Biol 63: 07TR01, 2018.
23. Galperin MY, Kristensen DM, Makarova KS, Wolf YI and Koonin EV: Microbial genome analysis: The COG approach. Brief Bioinform 20: 1063-1070, 2019.
24. Stockman MC, Thomas D, Burke J and Apovian CM: Intermittent fasting: Is the wait worth the weight? Curr Obes Rep 7: 172-185, 2018.
25. Golbidi S, Daiber A, Korac B, Li H, Essop MF and Laher I: Health benefits of fasting and caloric restriction. Curr Diab Rep 17: 123, 2017.
26. Napoleao A, Fernandes L, Miranda C and Marum AP: Effects of calorie restriction on health span and insulin resistance: Classic calorie restriction diet Vs. Ketosis-Inducing diet. Nutrients 13: 1302, 2021.
27. Choi IY, Piccio L, Childress P, Bollman B, Ghosh A, Brandhorst S, Suarez J, Michalsen A, Cross AH, Morgan TE, *et al*: A diet mimicking fasting promotes regeneration and reduces autoimmunity and multiple sclerosis symptoms. Cell Rep 15: 2136-2146, 2016.
28. Wahl D, Solon-Biet SM, Wang QP, Wali JA, Pulpitel T, Clark X, Raubenheimer D, Senior AM, Sinclair DA, Coone GJ, *et al*: Comparing the effects of low-protein and high-carbohydrate diets and caloric restriction on brain aging in mice. Cell Rep 25: 2234-2243 e6, 2018.
29. Ikizler TA, Robinson-Cohen C, Ellis C, Headley SAE, Tuttle K, Wood RJ, Evans EE, Milch CM, Moody KA, Germain M, *et al*: Metabolic effects of diet and exercise in patients with moderate to severe Ckd: A randomized clinical trial. J Am Soc Nephrol 29: 250-259, 2018.
30. Kraus WE, Bhapkar M, Huffman KM, Pieper CF, Das SK, Redman LM, Villareal DT, Rochon J, Roberts SB, Ravussin E, *et al*: 2 years of calorie restriction and cardiometabolic risk (Calerie): Exploratory outcomes of a multicentre, phase 2, randomised controlled trial. Lancet Diabetes Endocrinol 7: 673-683, 2019.
31. Pak HH, Haws SA, Green CL, Koller M, Lavarias MT, Richardson NE, Yang SE, Dumas SN, Sonsalla M, Bray L, *et al*: Fasting drives the metabolic, molecular and geroprotective effects of a calorie-restricted diet in mice. Nat Metab 3: 1327-1341, 2021.
32. Tang Z, Ming Y, Wu M, Jing J, Xu S, Li H and Zhu Y: Effects of caloric restriction and rope-skipping exercise on cardiometabolic health: A pilot randomized controlled trial in young adults. Nutrients 13: 3222, 2021.
33. Sbierski-Kind J, Grenkowitz S, Schlickeiser S, Sandforth A, Friedrich M, Kunkel D, Glauben R, Brachs S, Mai K, Thürmer A, *et al*: Effects of caloric restriction on the gut microbiome are linked with immune senescence. Microbiome 10: 57, 2022.
34. Matson V, Chervin CS and Gajewski TF: Cancer and the microbiome-influence of the commensal microbiota on cancer, immune responses, and immunotherapy. Gastroenterology 160: 600-613, 2021.
35. Park EM, Chelvanambi M, Bhutiani N, Kroemer G, Zitvogel L and Wargo JA: Targeting the gut and tumor microbiota in cancer. Nat Med 28: 690-703, 2022.
36. Lu Y, Yuan X, Wang M, He Z, Li H, Wang J and Li Q: Gut microbiota influence immunotherapy responses: mechanisms and therapeutic strategies. J Hematol Oncol 15: 47, 2022.
37. Kim CS, Cha L, Sim M, Jung S, Chun WY, Baik HW and Shin DM: Probiotic Supplementation improves cognitive function and mood with changes in gut microbiota in community-dwelling older adults: A randomized, double-blind, placebo-controlled, multicenter trial. J Gerontol A Biol Sci Med Sci 76: 32-40, 2021.
38. Sergeev IN, Aljutaily T, Walton G and Huarte E: Effects of synbiotic supplement on human gut microbiota, body composition and weight loss in obesity. Nutrients 12: 222, 2020.
39. Kang DW, Adams JB, Coleman DM, Pollard EL, Maldonado J, McDonough-Means S, Caporaso JG and Krajmalnik-Brown R: Long-term benefit of microbiota transfer therapy on autism symptoms and gut microbiota. Sci Rep 9: 5821, 2019.
40. Ley RE, Backhed F, Turnbaugh P, Lozupone CA, Knight RD and Gordon JI: Obesity alters gut microbial ecology. Proc Natl Acad Sci U S A 102: 11070-11075, 2005.
41. Locantore P, Del Gatto V, Gelli S, Paragliola RM and Pontecorvi A: The interplay between immune system and microbiota in osteoporosis. Mediators Inflamm 2020: 3686749, 2020.
42. Cho I and Blaser MJ: The human microbiome: At the interface of health and disease. Nat Rev Genet 13: 260-270, 2012.
43. Human Microbiome Project Consortium: Structure, function and diversity of the healthy human microbiome. Nature 486: 207-214, 2012.
44. Li MM, Zhou Y, Zuo L, Nie D and Li XA: Dietary fiber regulates intestinal flora and suppresses liver and systemic inflammation to alleviate liver fibrosis in mice. Nutrition 81: 110959, 2021.
45. Stojanov S, Berlec A and Strukelj B: The influence of probiotics on the firmicutes/bacteroidetes ratio in the treatment of obesity and inflammatory bowel disease. Microorganisms 8: 1715, 2020.

46. Magne F, Gotteland M, Gauthier L, Zazueta A, Pesoa S, Navarrete P and Balamurugan R: The firmicutes/bacteroidetes ratio: A relevant marker of gut dysbiosis in obese patients? Nutrients 12: 1474, 2020.
47. Xia T, Duan W, Zhang Z, Li S, Zhao Y, Geng B, Zheng Y, Yu J and Wang M: Polyphenol-rich vinegar extract regulates intestinal microbiota and immunity and prevents alcohol-induced inflammation in mice. Food Res Int 140: 110064, 2021.
48. Stoeva MK, Garcia-So J, Justice N, Myers J, Tyagi S, Nemchek M, McMurdie PJ, Kolterman O and Eid J: Butyrate-producing human gut symbiont, clostridium butyricum, and its role in health and disease. Gut Microbes 13: 1-28, 2021.
49. Fujio-Vejar S, Vasquez Y, Morales P, Magne F, Vera-Wolf P, Ugalde JA, Navarrete P and Gotteland M: The gut microbiota of healthy chilean subjects reveals a high abundance of the phylum verrucomicrobia. Front Microbiol 8: 1221, 2017.
50. Jin H and Zhang C: High fat high calories diet (HFD) increase gut susceptibility to carcinogens by altering the gut microbial community. J Cancer 11: 4091-4098, 2020.
51. Lindenberg F, Krych L, Fielden J, Kot W, Frøkiær H, van Galen G, Nielsen DS and Hansen AK: Expression of immune regulatory genes correlate with the abundance of specific Clostridiales and Verrucomicrobia species in the equine ileum and cecum. Sci Rep 9: 12674, 2019.
52. Wu S, Zhang Y, Ma J, Liu Y, Li W, Wang T, Xu X, Wang Y, Cheng K and Zhuang R: Interleukin-6 absence triggers intestinal microbiota dysbiosis and mucosal immunity in mice. Cytokine 153: 155841, 2022.
53. Bindels LB, Beck R, Schakman O, Martin JC, Backer FD, Sohet FM, Dewulf EM, Pachikian BD, Neyrinck AM, Thissen JP, et al: Restoring specific lactobacilli levels decreases inflammation and muscle atrophy markers in an acute leukemia mouse model. PLoS One 7: e37971, 2012.
54. Bindels LB, Porporato P, Dewulf EM, Verrax J, Neyrinck AM, Martin JC, Scott KP, Calderon PB, Feron O, Muccioli GG, et al: Gut microbiota-derived propionate reduces cancer cell proliferation in the liver. Br J Cancer 107: 1337-1344, 2012.
55. Lin C, Cai X, Zhang J, Wang W, Sheng Q, Hua H and Zhou X: Role of gut microbiota in the development and treatment of colorectal cancer. Digestion 100: 72-78, 2019.
56. Zitomersky NL, Coyne MJ and Comstock LE: Longitudinal analysis of the prevalence, maintenance, and IgA response to species of the order Bacteroidales in the human gut. Infect Immun 79: 2012-2020, 2011.
57. Machiels K, Joossens M, Sabino J, Preter VD, Arijs I, Eeckhaut V, Ballet V, Claes K, Immerseel FV, Verbeke K, et al: A decrease of the butyrate-producing species Roseburia hominis and Faecalibacterium prausnitzii defines dysbiosis in patients with ulcerative colitis. Gut 63: 1275-1283, 2014.
58. Hou YP, He QQ, Ouyang HM, Peng HS, Wang Q, Li J, Lv XF, Zheng YN, Li SC, Liu HL and Yin AH: Human gut microbiota associated with obesity in chinese children and adolescents. Biomed Res Int 2017: 7585989, 2017.
59. Zeng Q, Li D, He Y, LiY, Yang Z, Zhao X, Liu Y, Wang Y, Sun J and Feng X: Discrepant gut microbiota markers for the classification of obesity-related metabolic abnormalities. Sci Rep 9: 13424, 2019.
60. Duncan SH, Hold GL, Barcenilla A, Stewart CS and Flint HJ: Roseburia intestinalis sp. nov., a novel saccharolytic, butyrate-producing bacterium from human faeces. Int J Syst Evol Microbiol 52: 1615-1620, 2002.
61. Tamanai-Shacoori Z, Smida I, Bousarghin L, Loreal O, Meuric V, Fong SB, Bonnaure-Mallet M and Jolivet-Gougeon A: Roseburia spp: A marker of health? Future Microbiol 12: 157-170, 2017.
62. Rajilic-Stojanovic M, Shanahan F, Guarner F and de Vos WM: Phylogenetic analysis of dysbiosis in ulcerative colitis during remission. Inflamm Bowel Dis 19: 481-488, 2013.
63. Takahashi K, Nishida A, Fujimoto T, Fujii M, Shioya M, Imaeda H, Inatomi O, Bamba S, Sugimoto M and Andoh A: Reduced abundance of butyrate-producing bacteria species in the fecal microbial community in crohn's disease. Digestion 93: 59-65, 2016.
64. Cayetano RDA, Park J, Kim GB, Jung JH and Kim SH: Enhanced anaerobic digestion of waste-activated sludge via bioaugmentation strategy-Phylogenetic investigation of communities by reconstruction of unobserved states (PICRUSt2) analysis through hydrolytic enzymes and possible linkage to system performance. Bioresour Technol 332: 125014, 2021.
65. Lu L, Zhao Y, Yi G, Li M, Liao C, Cho C, Zhang B, Zhu J, Zou K and Cheng Q: Quinic acid: A potential antibiofilm agent against clinical resistant Pseudomonas aeruginosa. Chin Med 16: 72, 2021.
66. Liang Q, Wang C and Li B: Metabolomic analysis using liquid chromatography/mass spectrometry for gastric cancer. Appl Biochem Biotechnol 176: 2170-2184, 2015.
67. Lee JH, Kim Y, Choi JW and Kim YS: Genetic variants and risk of gastric cancer: A pathway analysis of a genome-wide association study. Springerplus 4: 215, 2015.
68. Ruiz-Maso JA, Macho NC, Bordanaba-Ruiseco L, Espinosa M, Coll M and Del Solar G: Plasmid rolling-circle replication. Microbiol Spectr 3: PLAS-0035-2014, 2015.
69. Armengaud J, Urbonavicius J, Fernandez B, Chaussinand G, Bujnicki JM and Grosjean H: N2-methylation of guanosine at position 10 in tRNA is catalyzed by a THUMP domain-containing, S-adenosylmethionine-dependent methyltransferase, conserved in Archaea and Eukaryota. J Biol Chem 279: 37142-37152, 2004.
70. Chen D, Jin D, Huang S, Wu J, Xu M, Liu T, Dong W, Liu X, Wang S, Zhong W, et al: Clostridium butyricum, a butyrate-producing probiotic, inhibits intestinal tumor development through modulating Wnt signaling and gut microbiota. Cancer Lett 469: 456-467, 2020.
71. Sugimura N, Li Q, Chu ESH, Lau HCH, Fong W, Liu W, Liang C, Nakatsu G, Su ACY, Coker O, et al: Lactobacillus gallinarum modulates the gut microbiota and produces anti-cancer metabolites to protect against colorectal tumourigenesis. Gut 71: 2011-2021, 2021.
72. Wong SH and Yu J: Gut microbiota in colorectal cancer: Mechanisms of action and clinical applications. Nat Rev Gastroenterol Hepatol 16: 690-704, 2019.
73. Perez-Lopez A, Behnsen J, Nuccio SP and Raffatellu M: Mucosal immunity to pathogenic intestinal bacteria. Nat Rev Immunol 16: 135-148, 2016.